COVER SHEET

NOTE:

- ***Please attach the signed copyright release form at the end of your paper and upload as a single 'pdf' file***
- ***This coversheet is intended for you to list your article title and author(s) name only***
- ***This page will not appear in the book or on the CD-ROM***

Title: **A data-driven Bayesian Ascent method for maximizing wind farm power production**

Authors (names are for example only): Jinkyoo Park
Soonduck Kwon
Kincho H. Law

PAPER DEADLINE: ****May 15, 2015****

PAPER LENGTH: ****8 PAGES MAXIMUM ****

Please submit your paper in PDF format. We encourage you to read attached Guidelines prior to preparing your paper—this will ensure your paper is consistent with the format of the articles in the CD-ROM.

NOTE: Sample guidelines are shown with the correct margins. Follow the style from these guidelines for your page format.

Hardcopy submission: Pages can be output on a high-grade white bond paper with adherence to the specified margins (8.5 x 11 inch paper. Adjust outside margins if using A4 paper). Please number your pages in light pencil or non-photo blue pencil at the bottom.

Electronic file submission: When making your final PDF for submission make sure the box at "Printed Optimized PDF" is checked. Also—in Distiller—make certain all fonts are embedded in the document before making the final PDF.

(FIRST PAGE OF ARTICLE)

ABSTRACT

This paper discusses a data-driven, cooperative strategy to maximize wind farm power production. By strategically coordinating the control actions of the wind turbines to actively mitigate the wake interference, the total wind farm power production can be improved for a given wind condition. To determine the optimum coordinated control actions of the wind turbines using only power measurements collected from the wind turbines, we employ the Bayesian Ascent (BA) method, a probabilistic data-driven optimization scheme. Wind tunnel experiments using 4 scaled wind turbine models have been conducted to validate (1) the effectiveness of the cooperative control strategy and (2) the efficiency of the BA algorithm in determining the optimum control actions of the wind turbines using only the power measurement data.

INTRODUCTION

As modern wind turbines now allow adjusting the blade angle, the yaw angle and the generator torque, this study investigates control strategies to maximize the power production of a wind farm. Currently, every individual wind turbine operates to maximize its own power production without taking into consideration the power productions of other wind turbines. Under this greedy control strategy, the wake formed by the upstream wind turbine would potentially lower the power productions of the downstream wind turbines due to the reduced wind speed and increased turbulence intensity inside the wake. Realizing that the interactions among the wind turbines can have impact on their power production, cooperative control strategies can be devised to maximize the total power production of a wind farm by manipulating the wake interference pattern.

To determine the optimum coordinated control actions of wind turbines, various approaches have been proposed. Mathematical models are constructed using the induction factor and the yaw-offset angle of a wind turbine as control inputs to adjust the wake interference pattern and thereby to increase the total energy production of a wind farm [1-5]. Optimization schemes, such as sequential convex programing, can be applied to optimize the coordinated control actions of wind turbines that maximize the

Jinkyoo Park and Kincho H. Law, Stanford University, CA 94305, U.S.A.
Soonduck Kwon, Chonbuk National University, Chonju-si, South Korea.

wind farm power function [6]. As alternatives to constructing wind farm power function, model-free optimization algorithms also have been applied to determine the optimum control actions. For examples, game theoretic search algorithm [7, 8] and the maximum power point tracking method [9] have been proposed to determine the optimum control actions using only the wind farm output data. For model-free methods, the strategy is to iteratively find better control actions by executing trial actions and observing the consequent power output. In this study, we have developed Bayesian Ascent (BA) method to expedite the iterative process in locating the optimum control actions. The method was tested previously through wind tunnel experiments with two scaled wind turbines by controlling the actions of the (single) upstream wind turbine [11]. In this work, we generalize the methodology to determine control actions for 4 scaled wind turbines. The objective is to study the effectiveness of the cooperative control approach and the scalability of the BA algorithm for optimizing wind farm power production with a number of wind turbines and varying wind directions.

BAYESAN ASCENT METHOD

For real-time, data-driven control, it is imperative that the control algorithm is able to improve the target value rapidly using a few measurement data. To achieve this goal, the Bayesian Ascent (BA) method is developed by incorporating into the Bayesian Optimization (BO) framework [11] strategies to regulate the search domain, analogues to a trust region in mathematical optimization [12]. The following briefly describe the BO framework and the sampling strategy for the BA method.

Bayesian Optimization

BO seeks to solve $\boldsymbol{x}^* = \arg\max_{\boldsymbol{x}} f(\boldsymbol{x})$ by iteratively choosing the input $\boldsymbol{x} = (x_1, \dots, x_i, \dots x_m)$, where m denotes the dimension of input $\boldsymbol{x}$, and observing the corresponding noisy response $y = f(\boldsymbol{x}) + \epsilon$, where ϵ represents the noise that is assumed to follow a Gaussian distribution [13]. The function $f(\boldsymbol{x})$, whose analytical expression is unknown, represents the model of the target system. To construct the unknown target function $f(\boldsymbol{x})$ in terms of its mean and variance, the BO process consists of two iterative phases, namely learning and optimization.

In the nth iteration of the learning phase, using the collected input data $\boldsymbol{x}^{1:n} = \{\boldsymbol{x}^1, \dots, \boldsymbol{x}^n\}$ and the observed output data $\boldsymbol{y}^{1:n} = \{y^1, \dots, y^n\}$, the unknown objective function $f(\boldsymbol{x})$ is modelled as a Gaussian Process (GP). In GP, the output value y^{n+1} of the target function for the unseen input $\boldsymbol{x}^{n+1}$ and the observed outputs $\boldsymbol{y}^{1:n} = \{y^1, \dots, y^n\}$ are assumed to follow a multivariate Gaussian distribution [14]:

$$\begin{bmatrix} \boldsymbol{y}^{1:n} \\ y^{n+1} \end{bmatrix} \sim N\left(\boldsymbol{0}, \begin{bmatrix} \mathbf{K} & \boldsymbol{k} \\ \boldsymbol{k}^T & k(\boldsymbol{x}^{n+1}, \boldsymbol{x}^{n+1}) \end{bmatrix}\right) \tag{1}$$

where $\boldsymbol{k}^T = \left(k(\boldsymbol{x}^1, \boldsymbol{x}^{n+1}), \dots, k(\boldsymbol{x}^n, \boldsymbol{x}^{n+1})\right)$ and $\mathbf{K}$ is the covariance matrix (kernel matrix) whose (i,j)th entry is $\mathbf{K}_{ij} = k(\boldsymbol{x}^i, \boldsymbol{x}^j)$. The value of the covariance function $k(\boldsymbol{x}^i, \boldsymbol{x}^j)$ quantifies the similarity between the two input vectors $\boldsymbol{x}^i$ and $\boldsymbol{x}^j$; the more the two vectors differ, the closer the value of the covariance becomes zero, meaning that they are not correlated in terms of their function values.

We use a squared exponential covariance function whose evaluation between two input vectors $\boldsymbol{x}^i$ and $\boldsymbol{x}^j$ is expressed as [15]:

$$k(\boldsymbol{x}^i, \boldsymbol{x}^j) = \sigma_s^2 \exp\left(-\frac{1}{2}(\boldsymbol{x}^i - \boldsymbol{x}^j)^T \mathrm{diag}(\boldsymbol{\lambda})^{-2}(\boldsymbol{x}^i - \boldsymbol{x}^j)\right) + \sigma_\epsilon^2 \delta_{ij} \tag{2}$$

which is described by the hyper-parameters $\{\sigma_s, \sigma_\epsilon, \boldsymbol{\lambda}\}$. The term σ_s^2 is referred to as the signal variance that quantifies the overall magnitude of the covariance value; σ_ϵ^2 is referred to as the noise variance that quantifies the level of noise assumed to exist in the observed output response; and $\boldsymbol{\lambda} = (\lambda_1, \dots, \lambda_i, \dots \lambda_m)$ is referred to as the characteristic length scales to quantify the relevancy of the input features in $\boldsymbol{x}$ for predicting the response y. A large length scale λ_i indicates weak relevance, while a small length scale λ_i implies strong relevance of the corresponding input feature x_i.

In GP, the posterior distribution on the hidden function value $f^{n+1} = f(\boldsymbol{x}^{n+1})$ for the unseen input $\boldsymbol{x}^{n+1}$ given the historical data $\boldsymbol{D}^n = \{(\boldsymbol{x}^i, y^i) | i = 1, \dots, n\}$ can be expressed as an 1-D Gaussian distribution $f^{n+1} \sim N(\mu(\boldsymbol{x}^{n+1}|\boldsymbol{D}^n), \mu(\boldsymbol{x}^{n+1}|\boldsymbol{D}^n))$ with the mean and variance functions expressed, respectively, as [15]

$$\mu(\boldsymbol{x}^{n+1}|\boldsymbol{D}^n) = \boldsymbol{k}^T (\mathbf{K})^{-1} \boldsymbol{y}^{1:n} \tag{3}$$

$$\sigma^2(\boldsymbol{x}^{n+1}|\boldsymbol{D}^n) = k(\boldsymbol{x}^{n+1}, \boldsymbol{x}^{n+1}) - \boldsymbol{k}^T (\mathbf{K})^{-1} \boldsymbol{k} - \sigma_\epsilon^2 \tag{4}$$

Here, $\mu(\boldsymbol{x}^{n+1}|\boldsymbol{D}^n)$ and $\sigma^2(\boldsymbol{x}^{n+1}|\boldsymbol{D}^n)$ are used as the functions for evaluating, respectively, the mean and the variance of the function value f^{n+1} corresponding to the unseen input data $\boldsymbol{x}^{n+1}$. (f^{n+1} is the predicted true function value for unseen $\boldsymbol{x}^{n+1}$, which is not observable during BA simulation.)

In the nth iteration of the optimization phase, the mean function $\mu(\boldsymbol{x}^{n+1}|\boldsymbol{D}^n)$ and the variance function $\sigma^2(\boldsymbol{x}^{n+1}|\boldsymbol{D}^n)$, that probabilistically represent the unknown target function $f(\boldsymbol{x})$, are used to select the next optimum input $\boldsymbol{x}^{n+1}$ in order to *learn* more about the target function as well as to *improve* the target value. One popular approach to determine the next optimum input $\boldsymbol{x}^{n+1}$ is to maximize the expected improvement function $\mathrm{EI}(\boldsymbol{x})$ expressed as [16]:

$$\boldsymbol{x}^{n+1} = \arg\max_{\boldsymbol{x}} \mathrm{EI}(\boldsymbol{x}) \triangleq \mathrm{E}[\max\{0, f(\boldsymbol{x}) - f^{max}\} \,|\boldsymbol{D}^n] \tag{5}$$

where $\max\{0, f(\boldsymbol{x}) - f^{max}\}$ is the improvement toward the maximum output compared with the maximum output f^{max} observed so far. By selecting $\boldsymbol{x}$ that maximizes $\mathrm{EI}(\boldsymbol{x})$, we can obtain either the improved target function value f^{n+1} or the updated target function with reduced uncertainty at the selected input point $\boldsymbol{x}^{n+1}$.

Bayesian Ascent (BA) method

The Bayesian Ascent (BA) method imposes a proximity constraint to Eq. (5) such that the next solution $\boldsymbol{x}^{n+1}$ is chosen near the best solution observed so far. The strategy that we employ is similar to imposing a trust region constraint in mathematical optimization [12]. Additionally, we strategically adjust the size of the trust region to expedite the rate of convergence to an optimum. In other words, the optimization phase of BO using the BA method is posed as a constrained optimization problem described as [11]:

$$\begin{aligned} &\underset{\boldsymbol{x}}{\text{maximize}} \quad \mathrm{E}[\max\{0, f(\boldsymbol{x}) - f^{max}\} \,|\boldsymbol{D}^n] \\ &\text{subject to} \quad \boldsymbol{x} \in \boldsymbol{T} \triangleq \{\boldsymbol{x} | \; \|x_i - x_i^{max}\|_2 < \tau_i \;\text{ for }\; i = 1, \dots, m\} \end{aligned} \tag{6}$$

The trust region $\boldsymbol{T}$ is defined as a hypercube with its center being $\boldsymbol{x}^{max}$ that produces the maximum target value f^{max} within the historical data $\boldsymbol{D}^n$; the ith component τ_i of $\boldsymbol{\tau} = (\tau_1, \dots, \tau_i, \dots, \tau_m)$ determines the range where the i th component x_i of $\boldsymbol{x} = (x_1, \dots, x_i, \dots, x_m)$ is being sampled next. Thus, the vector $\boldsymbol{\tau}$ controls the overall size of the hypercube trust region where the exploration takes place. Furthermore, the size of the trust region is adjusted by scaling $\boldsymbol{\tau}$ during the iterations of BA. Imposing trust region and adjusting its size are to ensure a monotonic increase in a target value and gradual convergence to an optimum. Details of the procedure have been described previously in [11].

EXPERIMENTAL WIND TUNNEL STUDY

This section describes an experimental study to validate (1) the effectiveness of the cooperative wind farm control strategy for improving the total wind farm power and (2) the efficiency of the BA algorithm for finding the optimum coordinated control actions using only the power measurement data.

Wind turbine model

The scaled wind turbine model, shown in Figure 1, is made of three aluminum blades with a length of 70 cm. The rotor diameter is 150 cm. The tower is made of a steel tube with a height of 100 cm. The blade pitch angles are controlled by a servomotor (Dynamixel-64T). As shown in Figure 1(b), the rotation of the servomotor is transformed into a linear motion to rotate the blade angles through a mechanical linkage. The rotation angles of the servomotor range from $0°$ to $70°$ which convert the blade pitch angles varying from $0°$ to $20°$ (albeit they are not related in a linear fashion). We use the rotation of the servomotor, instead of the actual blade pitch angle, as the control variable for optimization. The rotational change of the servomotor is easy to track using the encoder in the servomotor, which is also used to acknowledge the executed control actions. As shown in Figure 1(b), the yaw angle is controlled by the same type of servomotor through a mechanical gear system. With an one-to-one gear ratio, the rotational angle of the servomotor is the same as the actual rotation of the yaw of the wind turbine. An AC generator, shown in Figure 1(b), is used to convert the mechanical energy into electrical energy.

Control board

Figure 2 shows the circuit board designed to measure the electrical power output from the wind turbine and to execute the control actions to adjust the blade and yaw angles of the wind turbine. The AC voltage output from the generator is converted into DC voltage by the rectifier. The rectified voltage and the associated current flowing through the load resistance are then measured using voltage and current sensors, from which the instantaneous power is computed. The microcontroller (Arbotix-M) continuously samples the instantaneous power and compute the average power (using a moving average technique). The microcontroller then transmits the computed average power to the central node (laptop computer) through the XBee radio module every 2 minutes. The BA method processes the average power collected from the wind turbines in the central node and determines the next control actions. The determined control actions are then wirelessly transmitted to the microcontroller to change the blade pitch and the yaw angle in the wind turbine.

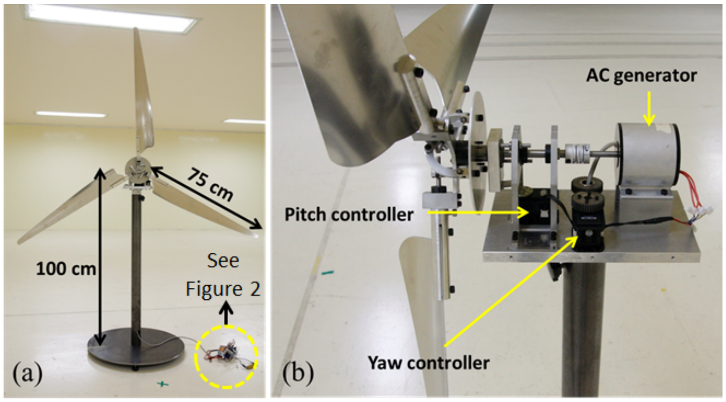

Figure 1. Scaled wind turbine model

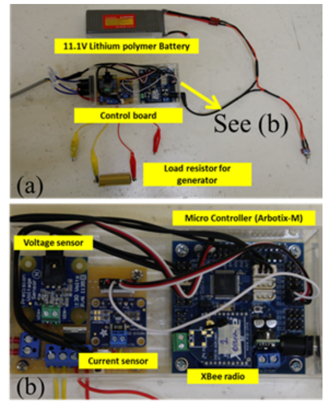

Figure 2. Control board

Configurations of wind tunnel experiments

Figure 3 shows the layout of the wind turbines in the wind tunnel experiments. The wind turbines are arranged in a linear pattern and separated by an inter distance of 7D ($= 10.5$ m). Using the linear wind farm layout, we study the effectiveness of the BA control algorithm and the effects of (1) the number of wind turbines (i.e., dimension of control variables) and (2) the wind direction on the cooperative control. Since the wind flow direction is fixed in the wind tunnel, the wind direction is emulated by changing the relative locations of the wind turbines. After changing the locations, the yaw angles of the wind turbines are set to be perpendicular to the wind direction. The constant wind speed of 3 m/s is used throughout the experiments. To evaluate the performance of the cooperative control approach and the BA algorithm, two reference wind turbine powers are measured for each experiment scenario:

- P_i^F: Freestream maximum power of wind turbine i that can be produced at a given location when there is no wake interference. The measured power P_i normalized by P_i^F then represents the power efficiency for wind turbine i. The total wind farm power efficiency is computed as $\sum_{i=1}^{N} P_i / \sum_{i=1}^{N} P_i^F$, where N is the number of wind turbines considered.
- P_i^G: Greedy maximum power of wind turbine i that can be produced at a given location when the upstream wind turbines are producing their maximum powers. The wind farm power efficiency for the greedy control strategy is then computed as $\sum_{i=1}^{N} P_i^G / \sum_{i=1}^{N} P_i^F$.

For cooperative control, the control actions for the greedy optimum are experimentally determined first, from which the BA proceeds to find the optimum coordinated control actions.

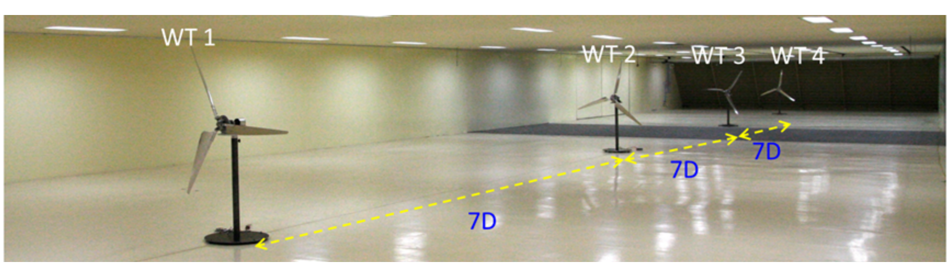

Figure 3. Layout of the wind turbines in the wind tunnel (KOCED Wind Tunnel Center in Chonbuk National University).

RESULTS

First, we study the application of cooperative control for 2, 3 and 4 wind turbines (i.e., $N = 2, 3$ and 4) when the wind turbines are initially directly facing the wind direction $\mathrm{WD} = 0°$. Figure 4 shows the trajectories of individual power efficiency P_i/P_i^F and the associated control actions of the wind turbines with the iterations of the BA algorithm. For cooperative control, the wind turbines collectively adjust their control actions determined by the BA algorithm to increase the total wind farm power production. As shown in Figure 4, cooperative control actions lower the power production for the first upstream wind turbine but significantly increase the power productions of the downstream wind turbines. For each case, the last downstream wind turbine operates at its greedy control actions since the deviation from the greedy control actions only decrease its own power production.

Figure 5 shows the improvement in the total wind farm power efficiency by the BA algorithm compared to the greedy wind farm power efficiency. As shown in the figure, BA increases the wind farm power efficiency almost monotonically. As shown in Figure 5, the initial wind farm power efficiency for the greedy control decreases as the number of wind turbine increases since a larger number of wind turbines are affected by wake influence. Furthermore, as the number of wind turbines increases, the relative improvement by the cooperative control actions increases but the number of iterations needed to reach the optimum also increases.

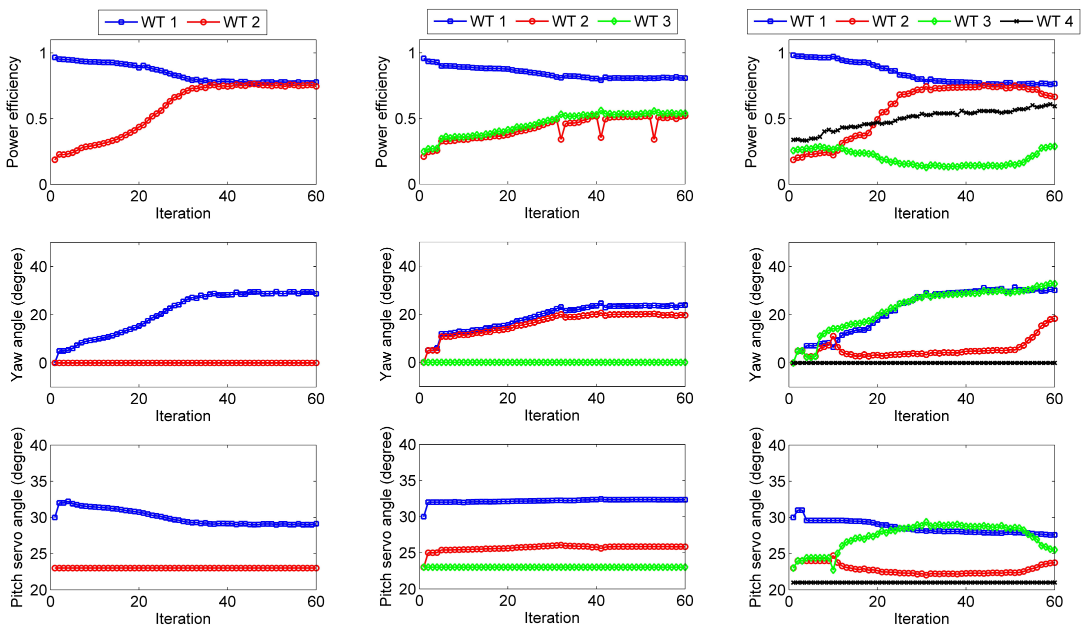

(a) No. of WTs = 2 (b) No. of WTs = 3 (c) No. of WTs = 4

Figure 4. Control actions and power efficiencies for different number of WTs.

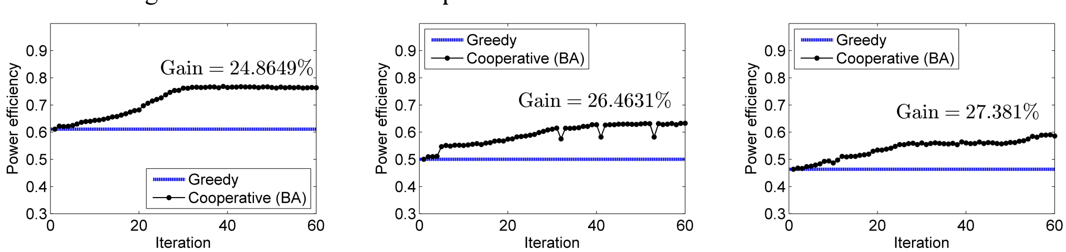

(a) No. of WTs = 2 (b) No. of WTs = 3 (c) No. of WTs = 4

Figure 5. Improvement on power production using cooperative control for different number of WTs.

Second, we study the effect of wind direction on the effectiveness of the cooperative control strategy using the BA algorithm. By varying the wind directions, WD = 0°, WD = 3° and WD = 6°, the BA algorithm is employed to optimize the coordinated control actions of 4 wind turbines. Figure 6 shows the trajectories of the control actions and the power efficiencies of the 4 wind turbines with the iterations of the BA algorithm. As shown in Figure 6(a), when the wind direction is 0° where the wake is perfectly aligned with the wind turbine array, the downstream wind turbines, WT 2, WT 3 and WT 4, initially produce only a small fraction of the power produced by the upstream wind turbine in the front. As the wind direction deviates from 0°, the downstream wind turbines are affected less by the wakes formed by the upstream wind turbines and, thus, produce more powers compared to the powers produced when WD = 0°.

As shown in Figure 7, the greedy wind farm power efficiency increases as the wind direction deviates from 0°. For example, when WD = 6°, the wind farm power efficiency is higher than 80% even before executing the cooperative control strategy. When the cooperative control strategy is employed, the wind farm power efficiency further increases. Note that the differences between the optimum power output and the initial (greedy) power production of the four wind turbines became smaller as the deviation of the wind direction from 0° increases.

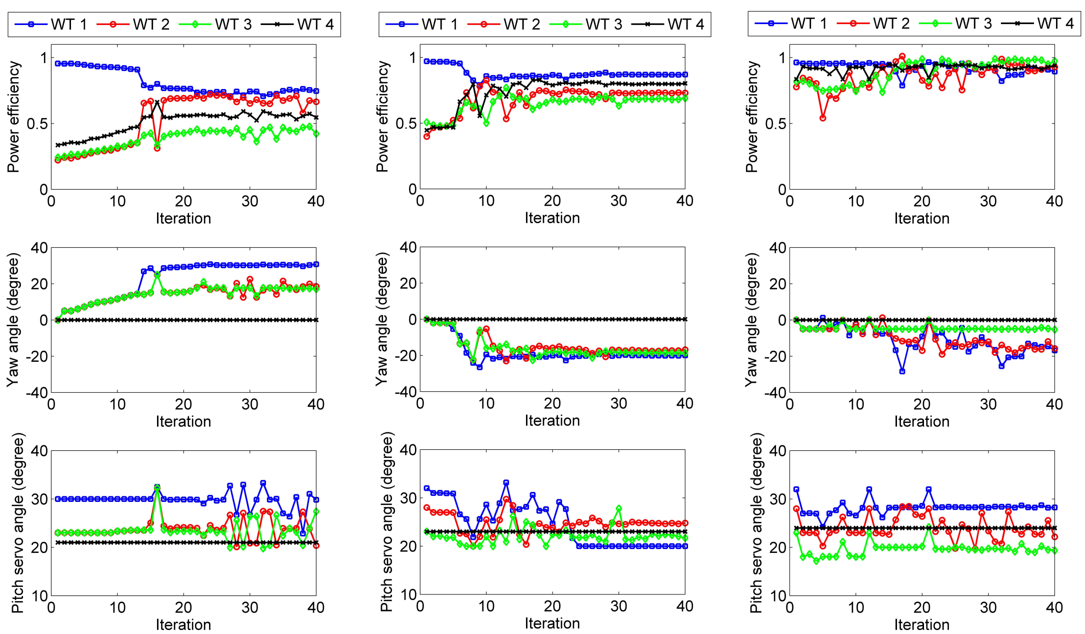

(a) WD = 0° (b) WD = 3° (c) WD = 6°

Figure 6. Control actions and power efficiencies for different wind directions.

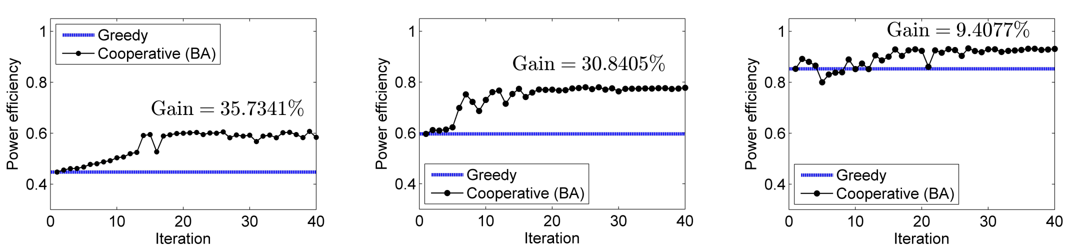

(a) WD = 0° (b) WD = 3° (c) WD = 6°

Figure 7. Improvement on power production using cooperative control for different wind directions.

DISCUSSIONS

The effectiveness of the cooperative control using the Bayesian Ascent method have been validated by conducting wind tunnel experiments with 4 scaled wind turbines. Results show that, for different number of wind turbines and wind directions, using the cooperative control approach, the total wind farm power production improves significantly as comparing to power production using the conventional control greedy control approach. By measuring the power outputs and executing the *trial* control actions, BA method is able to find optimum coordinated control actions of the wind turbines using a small number of iterations. The proximity constraint imposed on the BA algorithm ensures that the total wind farm power efficiency increases monotonically by gradually changing the control actions, i.e., the yaw and the blade pitch angles. It should be emphasised that in general the amount of power improvement that can be achieved through the optimization depends on the types of wind turbines (e.g., blade shape and generator) and the wind flow conditions, e.g., turbulence level.

REFERENCES

1. Johnson, K. and Thomas, N. 2009. “Wind farm control: addressing the aerodynamic interaction among wind turbines,” *Proceedings of the American Control Conference*, St. Louis, MO.
2. Madjidian, D. and Ranter, A. 2011. “A stationary turbine interaction model for control wind farms,” *Proceedings of 18th World Congress of the International Federation of Automatic Control*, Milano, Italy, pp. 4921–4926.
3. Bitar, E. and Seilter, P. 2013. “Coordinated control of a wind turbine array for power maximization,” *Proceedings of the American Control Conference*, Washington, D.C.
4. Wagenaar, J., Machielse, L., and Schepers, J. 2012. “Controlling wind in ECN’s scaled wind farm,” *Proceedings of Europe Premier Wind Energy Event*, pp.685–694.
5. Dahlberg, J. and Medici, D. 2003. “Potential improvement of wind turbine array efficiency by active wake control,” *Proceedings of European Wind Energy Conference*, pp.65–84.
6. Park, J. and Law, K. 2015. “Cooperative wind turbine control for maximizing wind farm power using sequential convex programming,” *Energy Conversion and Management* (in press).
7. Marden, J., Ruben, S. and Pao, L. 2013. “A model-free approach to wind farm control using game theoretic methods,” *IEEE Transactions on Control Systems Technology*, 21(4), pp. 1207-1214.
8. Gebraad, P.M.O., Teeuwisse, F., Wingerden, J. W., Fleming, P., Ruden, S., Marden, J. and Pao, L. 2014. “Wind plant power optimization through yaw control using a parametric model for wake effects-a CFD simulation study,” *Wind Energy*, DOI: 10.1002/we.1822.
9. Gebraad, P. M. O. and Wingerden, J. W. 2015. “Maximum power-point tracking control for wind farms,” *Wind Energy*, 18(3), pp. 429-447.
10. Fleming, P., Gebraad, P, Lee, S., Wingerden, J., Johnson, K., Churchfield, M. and Moriarty, P. 2014. “Simulation comparison of wake mitigation control strategies for a two-turbine case,” *Wind Energy*, DOI: 10.1002/we.1810.
11. Park, J. and Law, K. 2015. “A Bayesian Ascent method for data-driven cooperative wind farm control,” *Proceeding of SPIE Smart Structures and Materials+Nondestructive Evaluation and Health Monitoring*, San Diego, CA.
12. Nocedal, J. and Wright, S. (2000). Numerical Optimization. Springer, New York.
13. Bronchu, E., Cora, M. V. and Freitas, N. 2010. “A tutorial on Bayesian optimization of expensive cost functions with application to active user modelling and hierarchical reinforcement learning,” Tech. Rep. arXiv:1012.2599, Department of Computer Science, University of British Columbia.
14. Rasmussen, C.E. and Williams, C.K. 2006. Gaussian processes for machine learning, MIT Press, Cambridge, MA.
15. Neal, R. M. (1996). Bayesian learning for neural networks, Springer-Verlag, New York, NY.
16. Mockus. J., Fretitas, A. and Castelanous, J. A. 1978. Towards global optimization, North-Holland, Amsterdam.

DEStech Publications, Inc.

CONTRIBUTING AUTHOR COPYRIGHT RELEASE FORM

As author of the chapter/contribution titled Bayesian Ascent method: An efficient data-driven optimization for maximizing wind farm power to appear in the *Proceedings of Structural Health Monitoring 2015*, I hereby agree to the following:

1. To grant to DEStech Publications, Inc., 439 North Duke Street, Lancaster, PA, 17602, copyright of the above named chapter/contribution (for U.S. Government employees to the extent transferable), in print, electronic, and online formats. However, the undersigned reserve the following:
a. All proprietary rights other than copyright, such as patent rights.
b. The right to use all or part of this article in future works.

DEStech Publications thereby retains full and exclusive right to publish, market, and sell this material in any and all editions, in the English language or otherwise.

1 I warrant to DEStech Publications, Inc., that I am the (an) author of the above-named chapter/contribution and that I am the (a) copyright holder of the above-named chapter/contribution granted to DEStech Publications, Inc.

2 I warrant that, where necessary and required, I have obtained written permission for the use of any and all copyrighted materials used in the above-named chapter/contribution. I understand that I am responsible for all costs of gaining written permission for use of copyrighted materials.

3 I agree to assume full liability to DEStech Publications, Inc. and its licensee, and to hold DEStech Publications, Inc. harmless for any claim or suit filed against DEStech Publications, Inc. for violation of copyrighted material used in the above-named contribution.

Please sign and date this form and retain a copy for your records. Please include original form with your chapter/paper.

Thank you for your cooperation.

Please print name: JinKyoo Park
Signed: ______ Dated: 31 May 2015

439 NORTH DUKE STREET • LANCASTER, PENNSYLVANIA 17602-4967, U.S.A. Toll Free: (866) 401-4337 • Tel: (717) 290-1660 • Fax: (717) 509-6100 E-mail: info@destechpub.com • Internet address: www.destechpub.com